SpectroCube: a European 6U nanosatellite spectroscopy platform for astrobiology and astrochemistry

Andreas Elsaesser[1], Fabrice Merenda[2], Robert Lindner[3], Roger Walker[3], Steeve Buehler[2], Gerben Boer[2], Andrés Villa[4], Yanina Hallak[4], Fernando Aguado[4], Edoardo Alberti[5], Brian Wood[5],*

[1]Department of Physics, Freie Universität Berlin, Arnimallee 14, 14195 Berlin, Germany, a.elsaesser@fu-berlin.de
[2]Arcoptix SA, Faubourg de la Gare 5a, 2000 Neuchâtel, Switzerland, merenda@arcoptix.com, buehler@arcoptix.com, boer@arcoptix.com
[3]European Space Agency ESA-ESTEC, Keplerlaan 1, 2200AG Noordwijk ZH, The Netherlands, roger.walker@esa.int, robert.lindner@esa.int
[4]Departamento Teoría de la Señal y Comunicaciones, Universidade de Vigo, 36310 Spain, andres.villa@space.uvigo.es, yanina.hallak@space.uvigo.es, faguado@tsc.uvigo.es
[5]Micos Engineering GmbH, Überlandstrasse 129, CH-8600, Dübendorf, Switzerland, edoardo.alberti@micos.ch, brian.wood@micos.ch
*Corresponding Author

Abstract

SpectroCube is a CubeSat-based miniaturized in-situ space exposure platform for astrochemistry and astrobiology research. Within a 6 unit (6U, with 1U corresponding to 10cm x 10cm x 10cm) nanosatellite structure, an infrared spectrometer is interfaced with a sample handling system to measure photochemical changes of organic molecules, representing important biomarkers for the detection of life in our solar system and beyond. Monitoring degradation profiles and photochemical reaction kinetics of such biomarkers allows to identify suitable search targets for current and future planetary exploration and life-detection missions. SpectroCube is designed to be launched into a highly elliptical orbit around Earth and therefore allows to expose samples to higher solar UV and energetic particle radiation levels than previous exposure platforms in low Earth orbit, as for example on the International Space Station. In-situ data will be telemetered back to Earth and compared with solar and planetary simulation experiments in ground-based laboratory. We here present the design of SpectroCube, the scientific payload and its subsystems. We demonstrate that with the miniaturisation potential of infrared spectroscope it is possible to fit the entire optical setup plus a sample handling system for up to 60 individually contained and hermetically sealed samples within less than half of the volume of a 6U CubeSat structure. Therefore, the remaining volume can be entirely used for additional subsystems such as attitude control, propulsion, fuel, onboard computer and telemetry.

The design of the scientific payload is based on a commercial off-the-shelf miniaturised Fourier-transform spectrometer consisting of an infrared light source, an interferometer and infrared detector units. The mechanical robustness and suitability of such a system for space applications was assessed. Shock and vibration testing of the mechanically most sensitive unit, the interferometer, was performed and revealed that with adequate damping the spectroscopic performance can be maintained. Additional measurements of test samples conducted with the selected commercial off-the-shelf spectrometer candidate showed that the spectroscopic range, resolution and sensitivity is capable to monitor *in situ* the photochemical kinetics of important classes of organic molecules and biomarkers for astrobiology and astrochemistry research.

Keywords: Astrochemistry; Astrobiology; In-situ monitoring; Fourier-transform infrared spectroscopy; CubeSat; highly elliptical Earth orbit

Acronyms/Abbreviations: Fourier-transform infrared (FTIR), ultraviolet (UV), commercial off-the-shelf (COTS), European Space Agency (ESA), National Aeronautics and Space Administration (NASA), deoxyribonucleic acid (DNA), International Space Station (ISS), geostationary transfer orbit (GTO), Mercury Cadmium Telluride (MCT), general environmental verification standard (GEVS), shock response spectrum (SRS), low Earth orbit (LEO)

1. Introduction

The effect of solar UV and energetic particle radiation on organic molecules is of great interest to the Astro/Exobiology and Astrochemistry research community with implications to cosmochemistry, the origin of life, and the search for life on other planets. Carbon-based molecules can be found ubiquitous in our galaxy [1, 2]. Their fate in the presence of electromagnetic and particle radiation could give clues to which biomolecules can form and persist in space and which molecules might have been delivered to the early earth or other planets in our solar system via meteoritic impact. Of particular interest is the photostability of biogenic molecules and specific biomarkers in the search for life beyond Earth and in preparation for ongoing and upcoming life-detection missions on other planets in our solar system such as Mars. Molecules that are potentially indicative for a biogenic origin include nucleobases, amino acids, fatty acids and other lipids. The latter are typically found as part of biological membranes. Cellular membranes are a key requirement in the origin and evolution of life and found in every life form on Earth. Their universal character together with their stability and longevity against environmental influences render them very important as biomarkers for future life-detection missions to other planets.

Two decades of successful experiments on the International Space Station (ISS) and on other platforms in low Earth orbit (LEO) have provided new information about the evolution of organic and biological material in space and planetary environments [3, 4]. A major limitation of past space exposure platforms was their ‘passive’ design, meaning no analytical capability for measuring experimental changes during the exposure period. Facilities and experiments with in-situ measurement capabilities are currently attracting the attention of the scientific community. Although technologically demanding and more complex in design and implementation, in-situ platforms are a highly promising new space experimentation tool.

The rapid advance in miniaturisation taking place in virtually every field of engineering including the space industry continues to boost the development of small satellites [5]. This includes miniaturisation of analytical instrumentation and space hardware and facilitates the design and development of small satellites and nanosatellites. CubeSats (defined as one or multiple units of cubes of 10 cm in length, width and height) have become an international standard for small satellites and further fuel the trend towards small, lightweight, low-power, cost-effective, modular space experiments, which are capable to return excellent science results. The CubeSat form factor is currently a quasi-standard for nanosatellites [6] and helped to promote these new space platforms to become highly modular and flexible both in terms of payload and launch/orbit configuration while at the same time reducing development time and manufacturing costs [7]. Nanosatellites were initially perceived as mainly an educational tool for students. However, in the last decade the development of nanosatellites with purely scientific payloads is ever increasing [8-10]. Not only academia but also space agencies and industry recognised the potential of nanosatellites for space sciences and research [11-13].

An apparent bottleneck in the development of nanosatellite projects with scientific objectives and research goals is the availability of miniaturised and space-ready analytical instrumentation.

Spectroscopic technology is particularly suited for in-situ measurements in space environments [14-16] due to its miniaturisation potential, light-weightiness of the hardware and minimum power requirements. Furthermore, spectroscopy is a non-destructive analytical method capable of investigating solid, liquid and gaseous samples by probing vibrational and rotational molecular bands. Spectroscopic technology (mainly in the UV-visible spectral region) has already proved highly successful in recently completed as well as ongoing space experiments on board of nanosatellites [17]. Attempts to expanding the spectroscopic range of miniaturised analytical hardware to the infrared spectrum have been made [18] and will allow probing important and highly specific molecular bands of key organic molecules such as amino acids, fatty acids or lipids. The mid-infrared spectral region (wavenumbers 3000-200cm^{-1}) is particularly suited to probe organic molecules with strong rotational and vibrational bands in the 4000-400cm^{-1} wavenumber region, in particular in the so-called fingerprint region (wavenumbers 1500-500cm^{-1}). Spectroscopic tools are highly attractive for scientific nanosatellite payload developments due to their inherent flexibility, analytical range and compatibility with a wide variety of samples and research targets. Furthermore, miniaturisation of spectrometers has greatly advanced in recent years and a variety of commercial systems are available. Modification of so-called commercial off-the-shelf (COTS) instruments for space applications is a highly promising way to develop scientific payloads for nanosats [16-18]. This approach reduced development time, costs and engineering risks and is, therefore, the preferred way for most current and future nanosat developments.

The 6U nanosatellite SpectroCube is an exposure platform, which will be able to monitor the photostability of organic compounds while being exposed to solar UV and energetic particle radiation beyond LEO. It will be equipped with a miniaturised Fourier-transform infrared spectrometer (FTIR) covering the mid-infrared spectrum (5000-800cm^{-1} wavenumber), a sample handling mechanism to measure spectra of up to 56 samples of organic molecules, which are of interest in the frame of searching for life beyond Earth. SpectroCube addresses the following key scientific objectives, which are focused on photostability assessment of organic molecules and potential biomarkers:

- To investigate photochemical pathways of organic molecules in space and planetary environments/atmospheres
- To elucidate the cause-effect relationship between UV/energetic particle radiation and organic molecule degradation (fragmentation and potential volatilisation)
- To establish a correlation between photostability and molecule properties
- To identify break-down patterns and degradation products, which could serve as highly specific biomarkers.

These objectives will be achieved by recording mid-infrared spectra of thin films and monolayers of organic molecules enclosed within hermetically sealed sample cells and irradiated via UV transparent windows, to study their degradation and reaction kinetics. The acquired data will be highly valuable for identifying organic molecules and potential biomarkers for future life-detection missions in our solar system and for astronomical observations. It will allow understanding better the response and survival of life to planetary and space conditions, not only with respect to habitability conditions but also in the context of planetary protection.

A design study conducted by the Concurrent Design Facility at the Technology Center of the European Space Agency (ESA-ESTEC, Noordwijk, NL) evaluated and assessed various designs and performed a trade-off analysis with respect to CubeSat size, orbit and mission duration while fulfilling the key scientific objectives of studying how the space environment beyond LEO impacts on life and its molecular building blocks.

With its modular design, the adaptation of COTS hardware and adherence to the CubeSat standard, SpectroCube embraces the CubeSat philosophy of modularity, reusability, adaptability and cost-effectiveness. The SpectroCube mission seeks to access harsh radiation environments beyond LEO on a low-cost nanosatellite platform, which is becoming a viable option due to upcoming launch opportunities as a piggyback payload. Furthermore, SpectroCube will provide a testbed for radiation hardened technologies for use on future deep space platforms and will be amongst the first deep space/interplanetary CubeSats with a scientific payload [19, 20].

2. SpectroCube

2.1 Mission Concept, Design and Specifications

SpectroCube is a 6-unit CubeSat (as illustrated in figure 1) with an approximate mass of 12 kg. SpectroCube fits entirely (including solar panels) within the volume envelope of a standard 6U CubeSat of 120x240x360mm [21]. The extended 6U-XL CubeSat format could be an additional option in case more volume is needed in the future. The scientific payload will occupy at least a third of the volume whereas the remaining two-thirds are reserved for attitude control, batteries, propulsion, communication and onboard computing. Besides the scientific payload with its in-situ infrared spectrometer and samples handling system, a UV and radiation dose sensor will be implemented as active instruments to monitor the radiation environment in orbit. UV photons from the sun are considered the main driver for photochemical changes of the selected organic samples. However, to discern the effects of particle and electromagnetic radiation, duplicates of samples are shielded from solar light but not from cosmic radiation. In this way, it is possible to monitor the effects of UV and particle radiation separately. Deployable solar panels cover nearly the entire outer surface of SpectroCube at launch. An inbuilt deorbiting mechanism will perform the necessary manoeuvres at the end of the scientific missions to comply with space debris mitigation requirements.

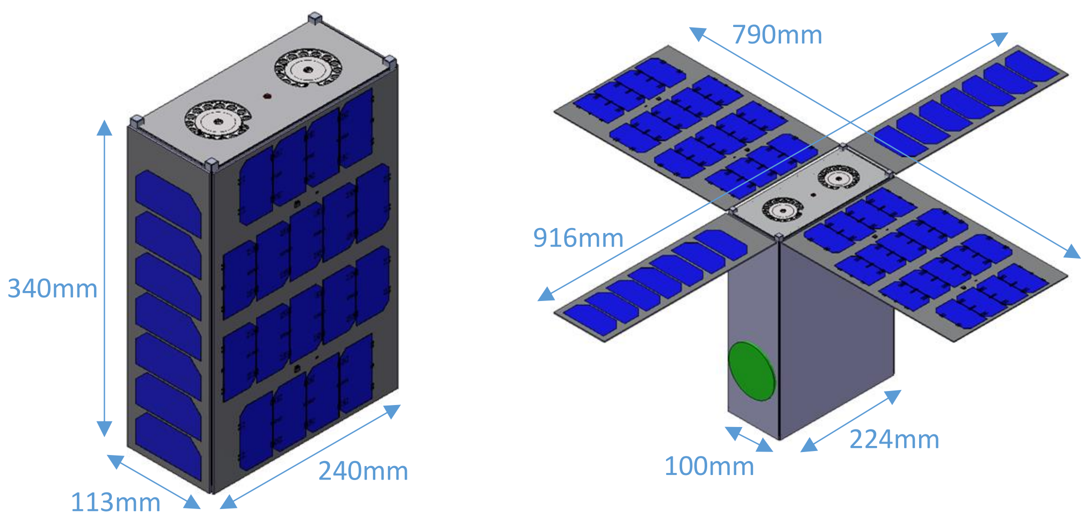

Figure 1: SpectroCube baseline design: 6U CubeSat with solar panels, propulsion, attitude control, antennas, thermal control, radiation sensors and scientific payload; left: launch configuration; right: flight configuration with deployed solar panels.

The internal distribution of the various subsystems of SpectroCube is shown in figure 2. The samples and the sample handling system of the scientific payload are placed at one of the 2U faces of the CubeSat to ensure optimal irradiation conditions. Underneath sit the interferometer, infrared light source and detectors together with all the required optical components to guide the infrared beam.

Additional systems in the centre of the CubeSat consist of the bus, control and communication system. Two S-band patch antennas are placed at the 3U side of the SpectroCube. The power subsystem consists of the solar panels, which are connected to an electrical power system for power generation, distribution and protection, battery packs and wiring to the subsystems requiring electrical power. An attitude control system consisting of four reaction wheels together with three magnetorquers consume nearly 2U and are mounted above the propulsion system. For redundancy, four cold gas thrusters with a range of 15 mN are seated at the 2U side opposite scientific payload at the bottom of the SpectroCube structure. The thrusters together with a propellant tank with nearly 0.3 L volume, a heater tank, temperature sensors and control unit represent the propulsion unit (see figure 2). To not inflate the mass of the CubeSat unnecessarily, radiation shielding is only added to radiation-sensitive components, mainly to the electronics of the science payload, communication and power subsystem. The expected total ionizing dose tolerance of most electronic components is approximately 20 kRad. A design study, which took into account various mission scenarios, considered 6 mm of aluminium shielding to be sufficient so that the total dose over the anticipated mission duration does not exceed 20 kRad.

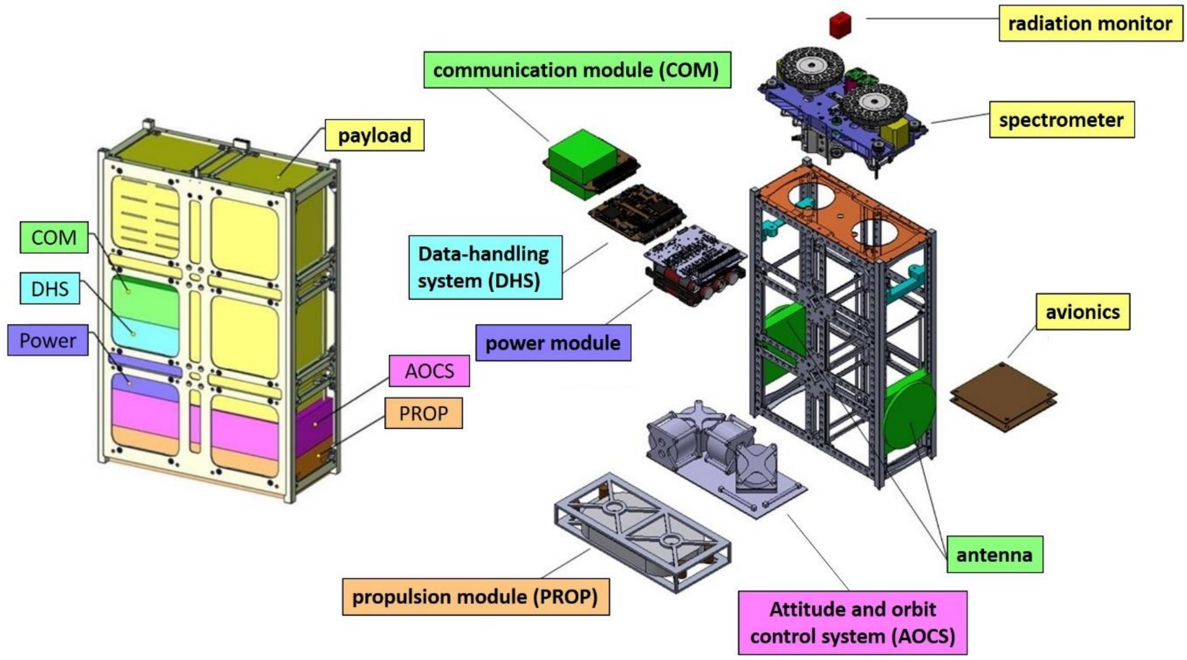

Figure 2: SpectroCube configuration and subsystems – on the left: 6U configuration with volume distribution of payload and subsystems; on the right: exploded view and individual components of SpectroCube.

Table 1 summarises the subsystems of the SpectroCube baseline design and lists key specifications and parameters for each. The final configuration and the internal volume distribution of the various subsystems depend on specific mission parameters such as mission duration, orbit configuration and radiation environment. A baseline mission scenario together with two alternative scenarios are discussed in the following.

Table 1: SpectroCube key parameters, subsystems and specifications.

SpectroCube Baseline Design Subsystems and Specifications	
Volume	6000cm^3
Mass	12kg
Density	2g/cm^3
Form Factor	Basic 6U structure

Subsystems	
Attitude, Orbit, Guidance, Navigation control subsystem	4 Reaction wheels of attitude control
	3 magnetorquers to de-saturate the reaction wheels
	Sun-sensors for pointing accuracy (5° half cone in nominal mode)
Propulsion	Cold gas propulsion module to raise or lower the orbit
Communication	S-band transceiver
Data handling	Redundant on-board computer
Power	Deployable solar panels (2x6U plus 2x3U)
Radiation	Shielding of the main electronic components to reduce locally the total ionising radiation dose to below 20 kRad (added weight by aluminium shielding with adequate thickness: ~648g)
Payload	2 sample carousels for housing up to 60 individual sample cells
	Low-power and compact infrared light source
	Interferometer
	Infrared detectors
	5 UV sensor (1x UV-A, 1x UV-B, 3x UV-C)
	Radiation sensor (electrons: 35 keV – 6 MeV, protons: 600 keV – 500 MeV, typical particle rate: $10^{-8}/cm^2/s$)

2.2 Orbit and Ground Stations

When the SpectroCube design and development process was initiated in 2015, a potential launch in 2020-22 was anticipated. The mission is expected to be completed within 6-12 months, depending on the actual radiation environment and the properties of the scientific samples. The total mission lifetime, during which scientific data is collected, is expected to last around 200 days. The post-mission lifetime for space debris mitigation will be less than 25 years. To expose scientific samples to the harsh radiation and space environment beyond LEO, SpectroCube is designed to be launched into a high Earth orbit with altitudes above 2000 km. Several orbit scenarios (Geostationary transfer orbit (GTO)/Molniya-type orbit, lunar swing-by, Sun-Earth Lagrange Point 2, Molniya orbit) have been identified together with suitable piggyback launch opportunities. A trade-off analysis of possible orbits considering launchers, ground station visibility, perigee/apogee altitude, eclipse duration and de-orbiting scenarios was conducted and led to the selection of the GTO/Ariane 5 orbit/launcher configuration as baseline, whereas super-GTO (sGTO)/Falcon 9 and Molniya /Soyuz/Fregat was seen as viable options (see figure 3).

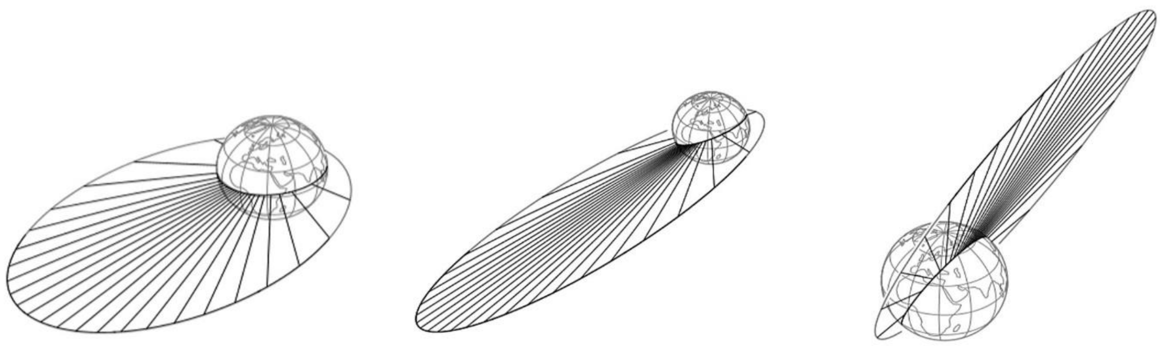

Figure 3: Possible SpectroCube orbits. left: Ariane 5 GTO; middle: Falcon 9 sGTO; right: Soyuz/Fregat Molniya.

Key parameters such as perigee, apogee, orbit duration and eclipse percentage are listed in table 2. GTO and Molniya type orbits will lead to fairly similar mission characteristics. The sGTO orbit is, on the other hand, due to its nearly doubled apogee distance, nearly twice as long. This has implications for the power budget and propulsion configuration. Nevertheless, the sGTO is scientifically highly interesting due to the expected higher levels of energetic particle radiation (electrons, protons, cosmic rays) at higher altitudes.

Table 2: Orbit and launcher configurations and specifications.

Orbit	Launcher	Perigee	Apogee	Orbit duration	Eclipse
GTO	Ariane 5	250 km	35786 km	10.5 h	14%
sGTO	Falcon 9	250 km	70000 km	23.4 h	15%
Molniya	Soyuz/Fregat	650 km	39732 km	12 h	8%

The selection of a GTO, sGTO or Molniya orbit will impact on the overall CubeSat design and will lead to differences in total mass (mainly caused by the differences in amount of propellant required), power budget and data storage (in a GTO and Molniya orbit, 5 scientific measurements will have to be stored in the onboard memory whereas for a SGTO orbit data storage for around 10 measurements need to be allocated due to the twice as long orbit). Table 3 summarises these differences and gives approximate values for each orbit. It should be noted that the mass budget of all orbit scenarios fulfils the mission requirements, after applying a 20% mass margin.

Table 3: Mass, data and power budget of the selected orbit scenarios.

Orbit	Mass (dry)	Mass (wet)	Mbit/orbit	Mbit/week (/day)	safe mode	commissioning mode	science mode (20% margin)
GTO	11.62kg	11.77kg	349	5563 (794)	8.9W	14.6W	28.8W (34.5)
sGTO	11.62kg	12.31kg	708	4988 (727)	8.9W	14.6W	25.9W (31.1)
Molniya	12.27kg	12.73kg	355	5091 (712)	8.9W	14.6W	25.2W (30.2)

Suitable ground stations were evaluated based on their availability, visibility, contact times, low variation and data rate. The communication windows with ground stations are defined to be between 10000 – 25000 km altitudes. The elevation is required to be at least 10°. For the close-to equatorial orbits four stations are considered, Malindi, Singapore, Panama and Hawaii (South Point), whereas the high inclination options include Kiruna and Svalbard. Table 4 lists the considered ground stations together with orbit/launcher dependent contact times and the time required to download the generated data (see table 3). For the latter, two cases were investigated: a spacecraft nominal pointing scenario with an antenna pointing angle of ±65° and a tumbling mode with an antenna pointing angle of ± 90°. Since data rate strongly depends on the distance between spacecraft and ground station, all calculations were based on a 30 000km range as a worst-case scenario. With an assumed onboard lossless compression of scientific data by 50%, all orbits have viable ground station network solutions with sufficient data rates and link budgets assuming a normal pointing mode. GTO and super-GTOs favour South Point Hawaii whereas the Kiruna ground station is best for the Molniya orbit. In a tumbling mode scenario, the combination GTO/South Point is possible whereas for the Molniya orbit the Kiruna ground station is best. With a sGTO orbit and a tumbling spacecraft none of the selected ground station combinations is feasible.

Table 4: Possible ground stations, contact times and feasible contact time duty cycle usage (normal and tumbling mode with 50% data compression).

	Contact times			Contact Time Duty Cycle Usage [%] (nominal/tumbling case)		
Ground station	Ariane 5 - GTO	Ariane 6/ Falcon 9 sGTO	Soyuz/ Fregat – Molniya	Ariane 5 - GTO	Ariane 6/ Falcon 9 sGTO	Soyuz/ Fregat – Molniya
Malindi	3.5	1.1	2.2	31.3/ -	90.3/ -	44.2/ -
South Point	3.4	1.1	2.7	19.3/60.9	49.9/ -	21.7/68.7
Kiruna	N.A.	N.A.	5	N.A./N.A.	N.A./N.A.	14.8/46.7

2.3 Science payload and sample configuration

SpectroCube's sample compartments for infrared measurements are cylindrical cells consisting of two windows separated by a spacer, shown in figure 4. Sample cell windows are made of Magnesium Fluoride (MgF_2), Calcium Fluoride (CaF_2) or Potassium Bromide (KBr) and the spacer material (typically stainless steel) can be adapted to the requirements of the experiment. Due to its excellent UV transmission properties, MgF_2 is currently considered the baseline window material. However, the selection of CaF_2 or KBr would improve the useable infrared wavelength range of sample measurements. The sample cell design is derived from the O/OREOS [15] and OREOcube [16] samples, which provides (in the case of O/OREOS) a proven TRL=9 hardware concept for sample enclosure.

The sample cells are 9mm in diameter and approximately 5mm thick, depending on the window thickness, with for example MgF_2 windows at the top and at the bottom, creating a fully enclosed reaction cell. Thin film samples are deposited as organic single/multilayers on for example the top MgF_2 window. The sample cells can also be filled with gaseous samples, thanks to the hermetically sealed sample design using an indium cold welding process. This ensures a leak rate of less than 6×10^{-10} mbar l/s [15] . Spectra of cells with no films and an IR-transparent gas such as nitrogen will serve as spectral blanks and references. Thin-film samples are prepared by vacuum deposition of high purity compounds onto the sample window. The cells, therefore, provide an internal environment that can house solid and gaseous samples or a combination thereof to study the influence of radiation exposure in situ.

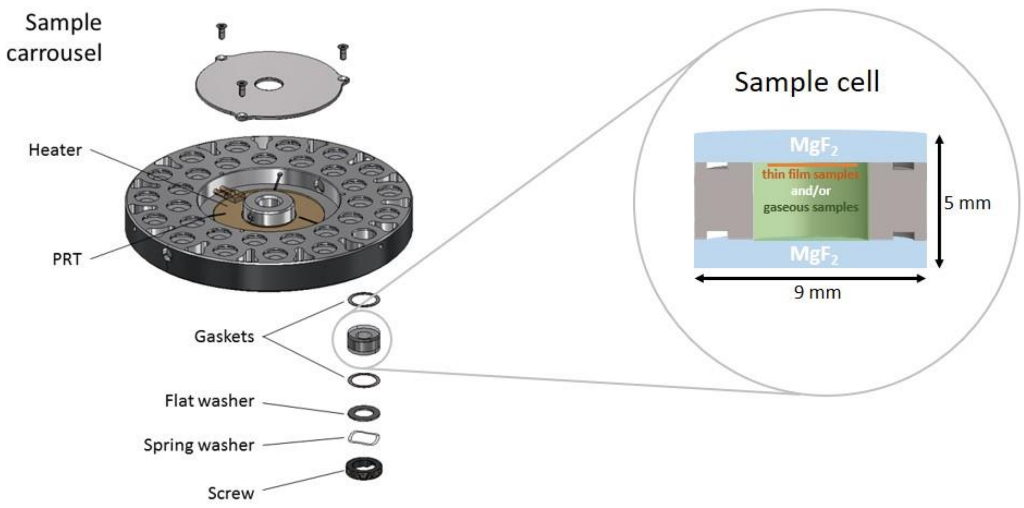

Figure 4: Left: Sample carrousel with 30 sample cell slots, showing details on heater and temperature sensor locations, as well as elements holding the sample cell in place (retaining ring, washers and gaskets); Right: cross-section of a sample cell showing its internal design (major components: top window, spacer, bottom window) with dimensions.

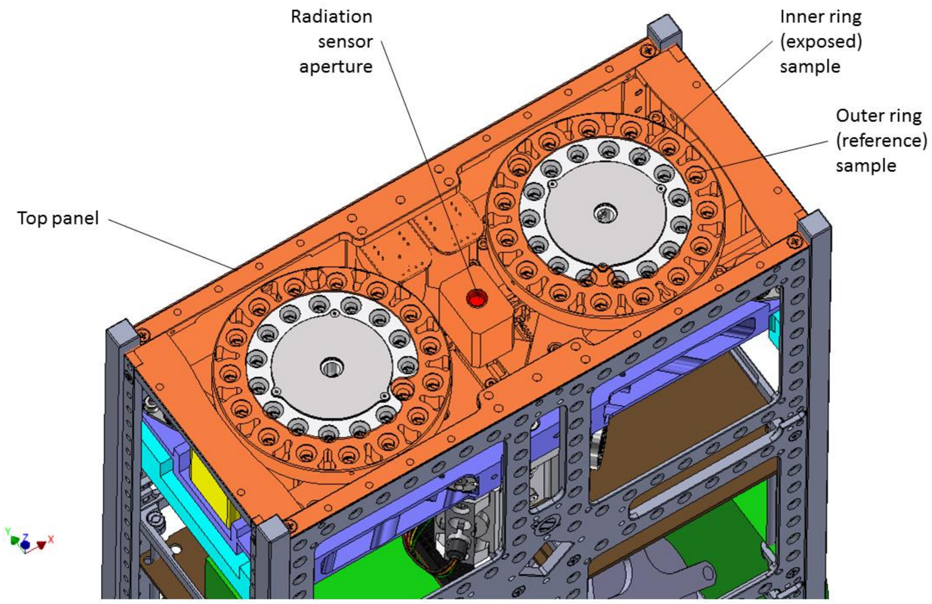

Figure 5: Detail of the top 2U side. Each of the two sample holding wheels includes two concentric rings of samples. Samples sitting in the outer rings are "reference" samples; they are shielded by the CubeSat top panel (its transparency is for illustration purposes only). Below the top panel also lies a radiation sensor.

The sample cells are held in two sample carrousels facing a 2U side of the CubeSat (see figure 5). The top CubeSat panel includes apertures that will leave exposed the samples located in the inner ring of each sample carousel while protecting from UV radiation reference samples that are in the outer rings. Each sample carrousel holds temperature sensors and a heater to monitor and control the temperature of the samples.

2.4 Spectrometer Configuration

The spectroscopic sub-systems of the SpectroCube are fixed on a single aluminium frame, as shown in figure 6. The heart of the payload is a miniaturised Fourier-transform infrared spectrometer (FTIR) manufactured by Arcoptix SA (Neuchâtel, Switzerland).

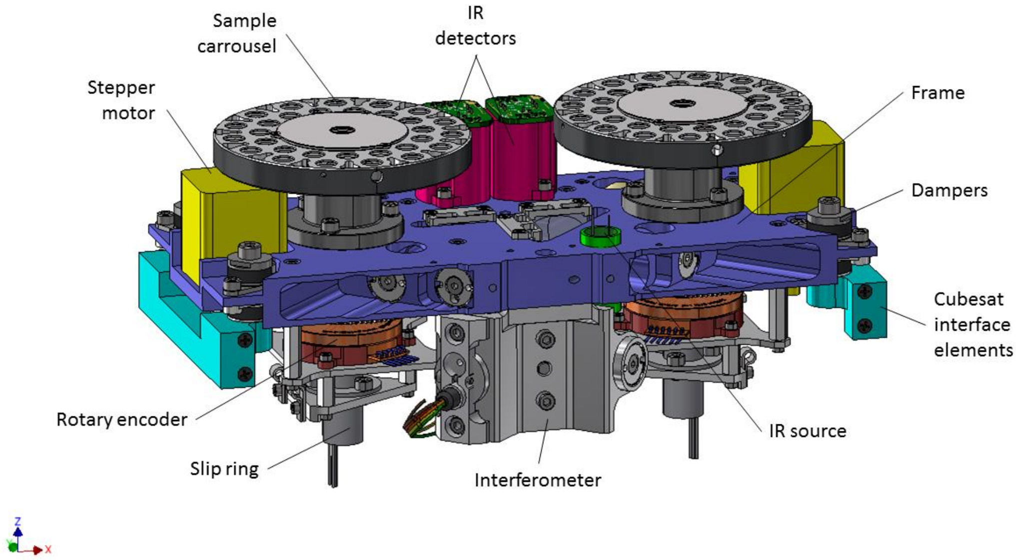

Figure 6: Spectrometer configuration. The FTIR and the two sample carrousel mechanisms are installed on a single frame, which is attached to the 6U CubeSat structure via dampers to protect the sensitive optics from launch vibrations and shocks.

The spectrometer consists of a Michelson interferometer (mounted below the frame), two infrared detectors (mounted on top of the frame), an infrared light source, as well as flat and parabolic mirrors and beamsplitters for IR beam-routing. The latter are mounted within the frame itself that includes holes to pass the infrared light beam. The two sample carrousel mechanisms are fixed to the frame on either side of the FTIR. The frame is fixed to the CubeSat structure via four dampers to protect the relatively fragile optical instrument from launch vibrations and shocks expected during the launch phase. The core of the FTIR is a customized version of the Arcoptix COTS interferometer, using two retroreflectors mounted on a pendulum. This is a proven, permanently aligned and self-compensated design [22-24] that is particularly robust against vibrations and shocks. The design is also very stable against temperature variations (better than 0.1 [%/K] @3000cm^{-1}) which is an important asset in view of temperature changes to be expected in orbit, in relation to the varying earth albedo and eclipses. The interferometer uses a ZnSe beamsplitter, has beam aperture of 12.7mm, and offers an unapodized resolution of 4cm^{-1}. The spectral range of the spectrometer unit is 5000-800cm^{-1}. Due to the use of MgF_2 windows as part of the sample compartment, the useable wavenumber range is 5000-1000cm^{-1}.

The two infrared detectors of the FTIR are thermo-electrically cooled MCT (Mercury Cadmium Telluride) detectors with optical immersion. The one order of magnitude improved detectivity compared to thermal detectors justifies the additional power needed for the thermo-electric cooling. Further details of sensitivity and spectral performance of the instrument are discussed in section 4.2.

The baselined infrared light source is a kanthal filament emitter. It can reach a temperature of almost 1200K with only 1.3W electrical power, thus emitting an intense and broadband black-body spectrum suitable for operation of the FTIR spectrometer.

All the infrared optics are lying below the sample wheels. In this way it can be ensured that no shadows from protruding parts are partly covering the sun exposed sample cells. The samples are measured in transflection mode, a configuration that is schematically illustrated in figure 7. The modulated IR beam coming out of the interferometer is focused into the sample cell through a beamsplitter and a parabolic mirror. A mirror placed on the opposite side of the sample reflects the IR light through the sample again. The beam coming back from the sample is then redirected to the IR detector by the beam-splitter.

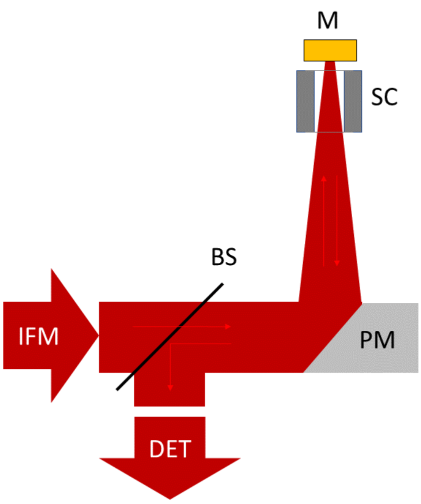

Figure 7: Schematic principle of transflection measurement. IFM: infrared beam coming from the interferometer. BS: beam-splitter, PM: parabolic mirror, SC: sample cell, M: mirror, DET: beam going to IR detector.

The actual implementation of the transflection configuration in the SpectroCube system (shown in figure 8) is more complex as it needs to route the beam to samples located in the left and right sample carrousels, and to the inner and outer sample rings of each sample carrousel. Light from the IR source (S) is collimated by a parabolic mirror (PM1) and is injected in the interferometer (IFM). After passing through the interferometer, the IR beam is brought up to the level of the main frame by two 90^{o} flat mirrors (M1 and M2). The IR beam then crosses a first beamsplitter (BS1) that shares the light onto the left and right sample carrousels. Two other beamsplitters (BS2) then divide the beam once more to distribute the light on two parabolic mirrors (PM2) that focus the IR beam through the samples located in the inner and outer rings of the sample carousel (SC). Note that when a sample of the inner ring is aligned with one of the parabolic mirrors PM2, the beam focused by the other parabolic mirror strikes in-between two sample cells of the outer ring, and vice versa. This ensures that only one sample per carrousel is probed at a time. After passing through a sample, the IR beam is reflected on the CubeSat top panel (TP) that has small portions of its inner side coated with gold. The light beam passes through the sample cell again, is re-collimated by the parabolic mirror (PM2), passes through the secondary beamsplitter (BS2) and is focused by another parabolic mirror (PM3) onto one of the IR detectors (D). Each sample carrousel has a dedicated IR detector, which allows measurements to be taken simultaneously from the two sample carrousels. Dedicated slots in the sample carousel with sample cells containing nitrogen or argon are reserved for reference measurements, which are used for recording of background spectra.

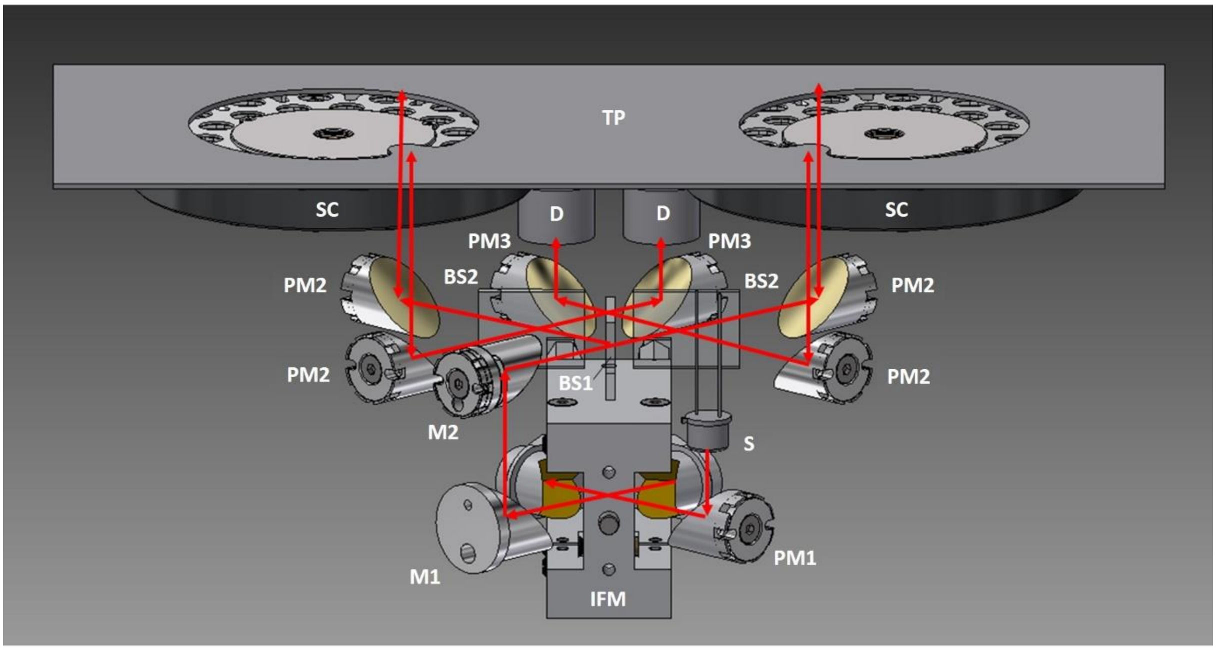

Figure 8: Schematic illustration of the IR beam path. See text for explanations.

To sequentially move each sample slot in the reading positions of the spectrometer optics the sample carrousels can rotate driven by stepper motors via 6:1 anti-backlash spur gears, as shown in Figure 9. The carrousels angular positions are permanently measured by individual rotary encoders, while the slip rings allow wiring of the temperature sensors and heaters located in the sample carrousels (see figure 4) via the hollow carrousel shafts.

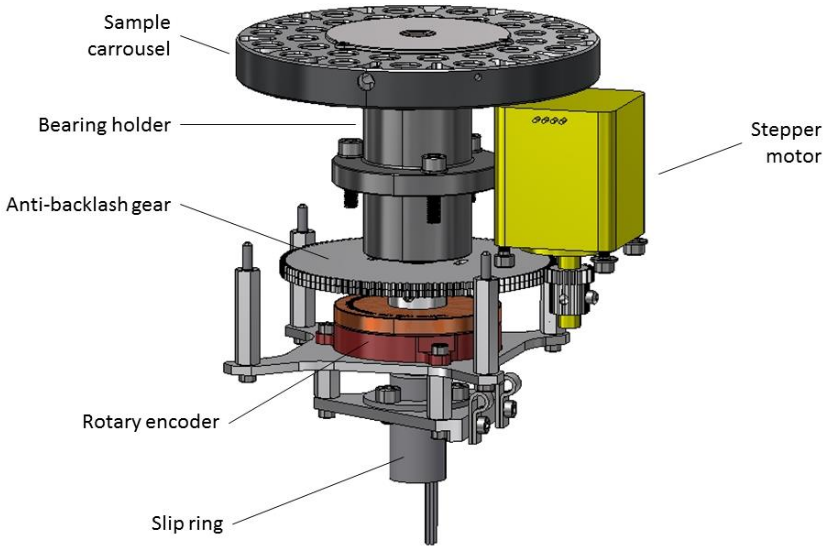

Figure 9: Details of the sample carrousel mechanism. See text for explanations.

3. Testing

3.1 Vibration and shock tests

The main objective of the first SpectroCube test campaign was to assess the robustness of the optical, mechanical and electrical COTS components of the interferometer against vibrations and mechanical shocks, while assessing its impact on the spectroscopic performance. Launch mechanical loads are of primary importance for SpectroCube as the FTIR payload is a particularly sensitive optical instrument. From a mechanical point of view, the interferometer is considered the most sensitive part of the scientific payload and misalignment due to shocks and vibrations could lead to significant deterioration of spectroscopic performance. The relative distance between certain optical elements must remain aligned to a fraction of wavelength, as otherwise the interferometer contrast – hence the data quality – would be drastically affected. Therefore, mounting of the instrument via dampers is foreseen. Random vibration and shock tests are the most threatening to the optical system, in link to the high frequency involved, which can create resonances on its small and rigid components. The random vibration power spectrum density (PSD) from the NASA General Environmental Verification Standard (GEVS) [25] is a well-established and conservative reference, and has been selected for the tests to be performed on the SpectroCube FTIR. The shock response spectrum (SRS) considered for testing is an envelope of the selected launchers, as given in table 5. The interferometer fringe visibility is measured before and after the random vibration and shock tests, as it is a fine indicator of its alignment.

Table 5 - SRS shock profiles of different launcher and with qualification margins.

	SRS [g]		
Frequency [Hz]	**Falcon 9**	**Soyuz & Ariane 5**	**MAX with margins (+3db)**
100	30	20	60
1000	1000	1000	2000
10000	1000	700	2000

3.2 Test samples

In addition to the vibration and shock testing, the overall spectroscopic performance of the COTS spectrometer was assessed based on measurements of fully assembled and representative gas-phase test samples, of which a subset was irradiated with UV photons simulating solar exposure. Gaseous samples carbon dioxide (CO_2) and methane (CH_4) exhibit characteristic and distinct infrared features, which are ideally suited to evaluate the spectroscopic performance of an FTIR spectrometer. Key parameters measured were signal-to-noise ratio, resolution, acquisition speed, repeatability and reproducibility.

4. Results and Discussion

4.1 Vibration and shock resistance

A small electromagnetic shaker from Brüel & Kjær (vibration exciter type 4809) was used to carry out the random vibration tests. The heart of the interferometer (see figure 8) was attached to the shaker in different orientations, as shown in figure 10. The accelerometer (a TE connectivity Model 64, 6000g version) was attached to the shaker-to-interferometer adapter plate.

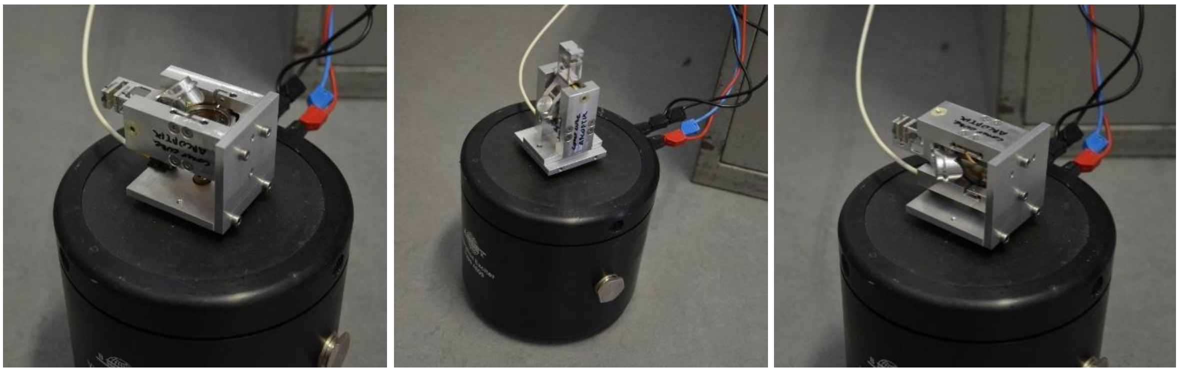

Figure 10: FTIR interferometer "heart" on the shaker in three different orientations (respectively X, Y and Z axes, corresponding to the axes shown in figure 5 and 6.

The shaker input signal was adjusted to produce an acceleration that simulates a GEVS random vibration PSD profile as "seen" by the payload through the dampers described in section 2.4. The dampers transmissibility was modelled as a 1st order system with an Eigenfrequency of $f_0 = 100Hz$ and a quality factor of $Q = 5$. The net effect of this simulated damping is to attenuate the high frequency vibration, at the cost of increasing frequencies closer to the resonance. Figure 11 shows the GEVS, target and recorded random vibration PSDs of the random vibration test. Some resonances can be distinguished in the random vibration spectra measured in the X and Z directions, which however did not result in any measurable reduction of the interferometer contrast.

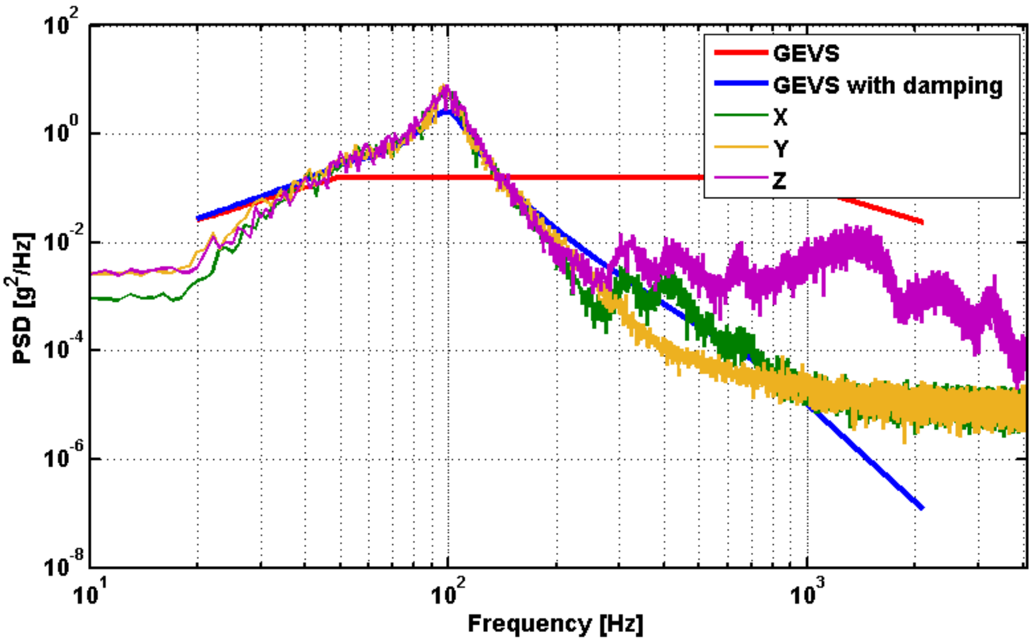

Figure 11: Random vibration test target and measured PSD profiles: GEVS with damping represents the test "target".

Shock testing was then performed with the hammer-based shock test system shown in figure 12, built following a design described by Jonsson [26]. A primary shock platform is directly hit by the hammer which allows testing direct shocks. A secondary platform can be mounted on top of the primary one via a system of dampers to mimic the shock attenuation by the payload dampers. The rigidity of the dampers was adjusted to reach a resonant frequency of 150Hz when the mass of the interferometer is included. Shock response spectra (SRS) were calculated from the accelerometer data based on a recursive formula presented by Smallwood [27].

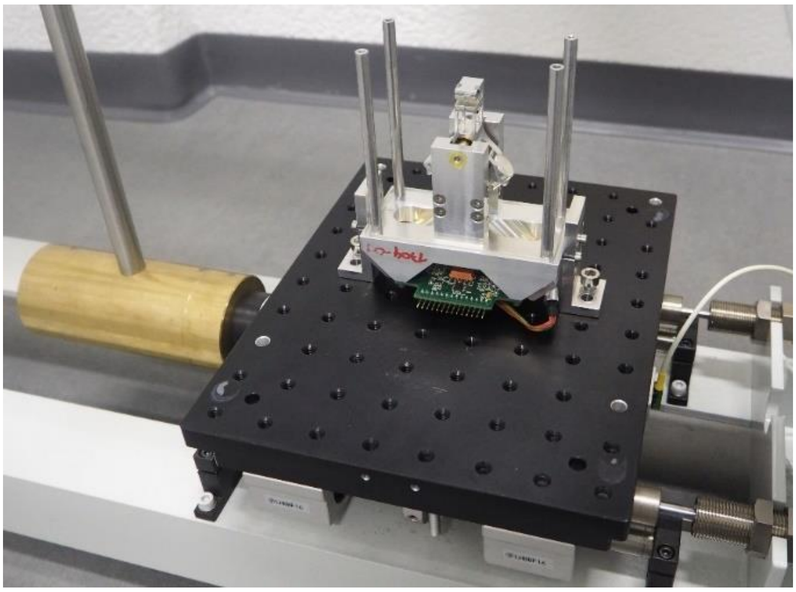

Figure 12: Hammer-based shock system used for testing the interferometer resistance to shocks.

A dummy mass - equivalent to the mass of the interferometer - was first installed on the secondary platform as the hammer height and impact element were adjusted to reach an SRS as specified in table 5 at the primary platform. The accelerometer was then alternatively installed on the upper and lower platforms. The SRS measured at both platforms are shown in figure 13.

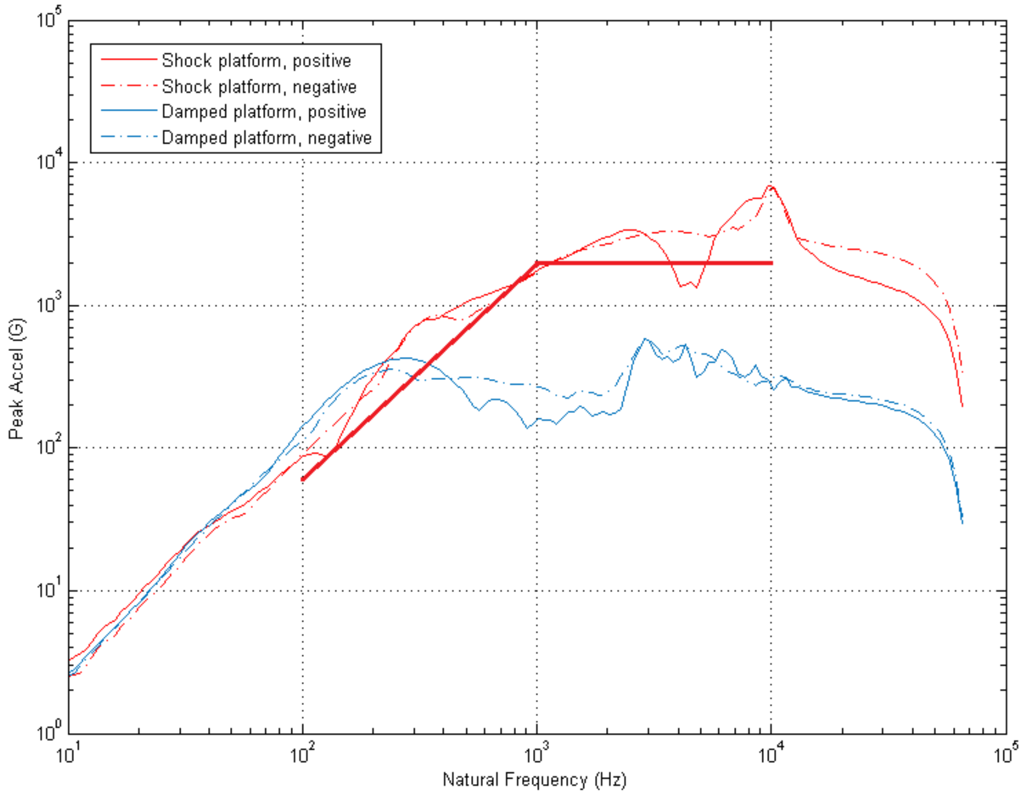

Figure 13: Acceleration shock response spectra SRS for Q=10 on direct shock platform (red) and damped platform (blue). The bold red line shows the target SRS level from table 5.

The measured shock response spectra demonstrate that the target levels specified in table 5 are reached at the primary (direct shock) platform. The dampers effectively protect the interferometer by attenuating the high-frequency shock, as measured on the secondary (damped shock) platform.

Before the test, the fringe visibility of the interferometer was measured to be 64.3 ± 0.2 %. After shocking the interferometer on the damped platform, in three orthogonal orientations, the fringe visibility was measured to be still 64.0 ± 0.2 %. These results show that the COTS FTIR can survive the expected random vibration and shock levels, provided that suitable damping is introduced. In fact, a similar shock test was carried out with the interferometer directly attached to the primary platform and submitted to the undamped SRS level shown on figure 13. The result was a plastic deformation of the beamsplitter holding clips and a total loss of the interferometer fringe visibility.

4.2 Spectroscopic performance

SpectroCube is designed to monitor *in situ* the photostability of organic molecules via infrared spectroscopy. Typical sample cells consist of thin films of organic molecules indicative for life. Organic molecules exhibit characteristic vibrational and rotational bands, especially in the so-called fingerprint region between 1500-500 cm^{-1} wavenumbers. As shown in figure 14, the spectrometer system of SpectroCube capable to resolve many features of candidate organic molecules, defined in the scientific objectives of the mission.

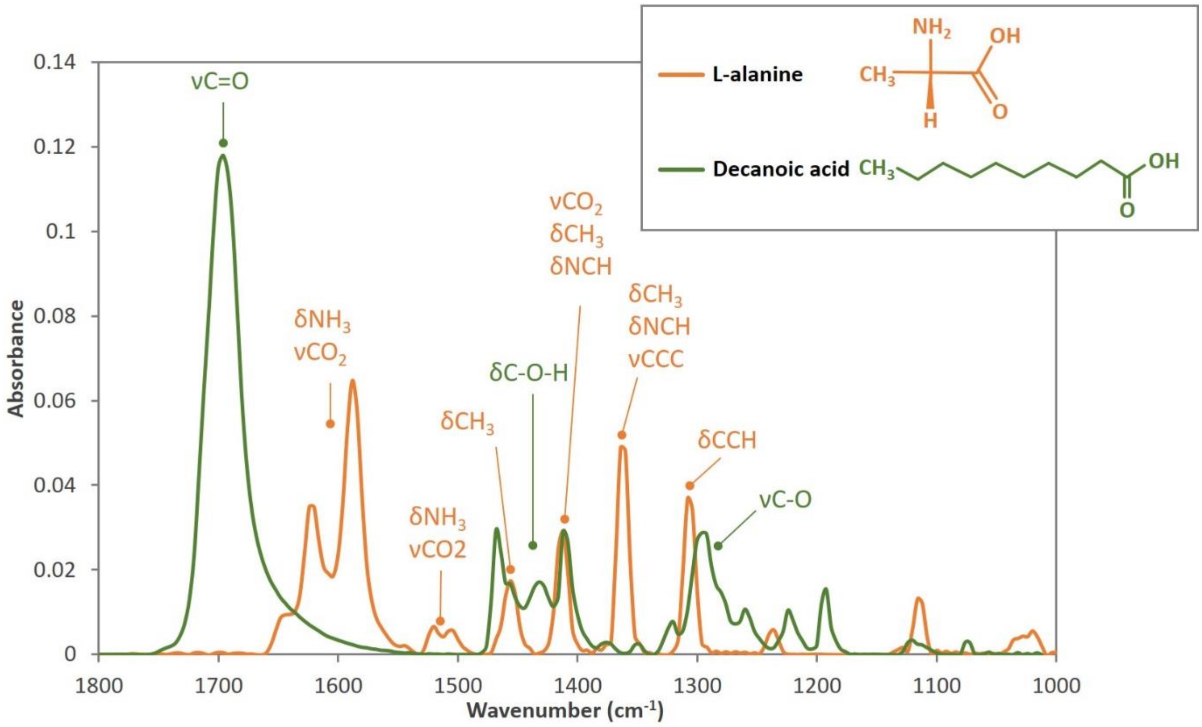

Figure 14: Thin film spectra of organic molecules recorded in the mid-infrared wavelength region with the COTS version of the SpectroCube spectrometer. Characteristic stretching (ν) and bending (δ) vibrations as reported in the literature [28, 29] are clearly visible and can be monitored over time.

In addition to the spectral information from the organic molecules, the gas atmosphere inside the sample cells can also be measured and monitored. Infrared spectra of specific gases are particular suited to test spectroscopic performance since gas molecules show much finer band structures than for example organic thin films. Methane and carbon dioxide are good examples for gas molecules with distinct mid-infrared features and are, furthermore, scientifically relevant due to their occurrence on for example Mars.

The methane molecule consists of 1 carbon atom and 4 hydrogen atoms attached to it via covalent bonds. Of the 9 fundamental modes of vibration of the methane molecule, 5 modes are degenerate due to the symmetry of the molecule. Of the remaining 4 fundamental modes, only 2 modes are infrared active. To test the spectral resolution of the spectroscopic system, we focused on the Q-, P- and R-branch of the v_3 fundamental mode at around 3020 cm^{-1}, see figure 15. A direct comparison with spectra taken on a state-of-the-art benchtop FTIR spectrometer (Bruker IFS66V) at $1cm^{-1}$ and $2cm^{-1}$ wavenumber resolution illustrates that spectral acquisition with $4cm^{-1}$ (maximum resolution of the SpectroCube spectroscopy unit) captures each of the side branches and the centre branch but does not fully resolve the individual modes of the Q- and R- branch.

A test study to investigate the photostability of a methane-filled sample cell demonstrated that the sample cells are leak tight under simulated radiation conditions. To confirm that the cells are hermetically sealed, the methane content was monitored in intervals of days and weeks without measuring any change in the spectroscopic signature. To demonstrate that photochemical changes could be observed, a subset of sample cells were irradiated for several hours with a standard Xenon arc lamp with significant contributions of UV photons in the 200-400nm region. With residual carbon and oxygen in the enclosed volume, the UV component of the light source produced measurable amounts of CO_2 inside the cells, see figure 16a and 16b.

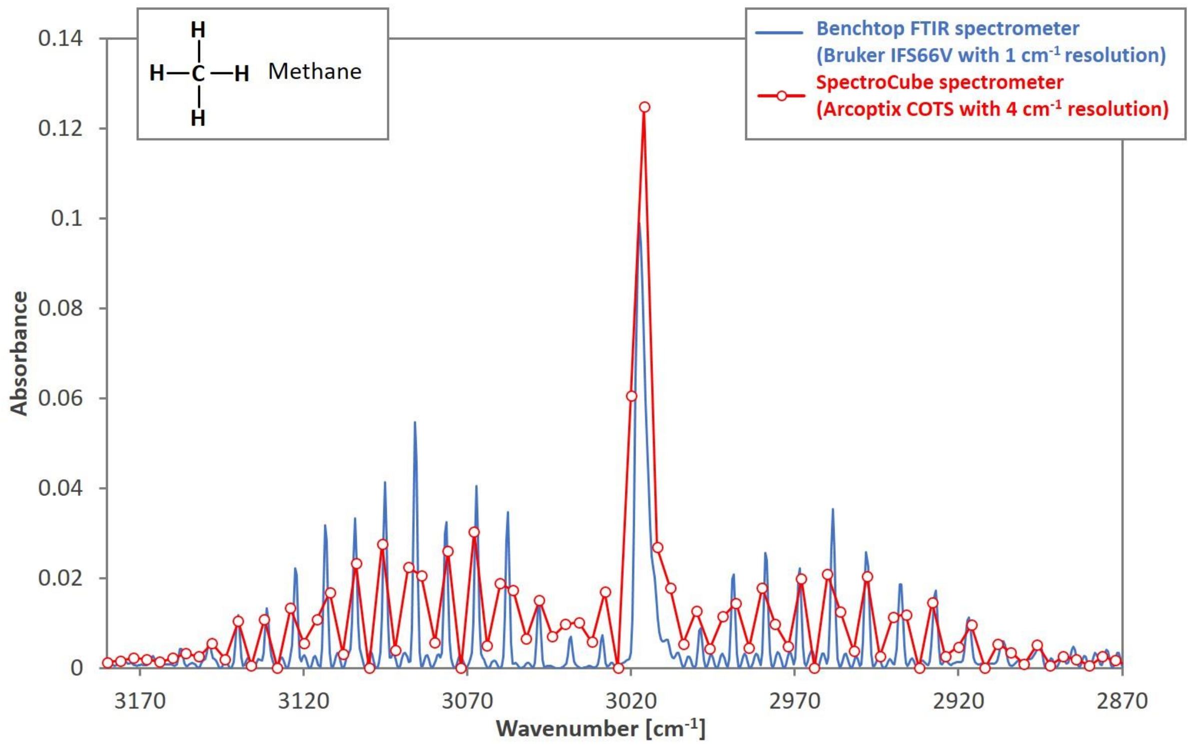

Figure 15: FTIR spectra of methane – gas cell with 5% methane in argon. Spectrum (blue) of the v_3 mode of methane recorded with a benchtop FTIR spectrometer (Bruker IFS66V) at a resolution of 1 cm^{-1} wavenumbers and direct comparison with a spectrum (red) of the same sample recorded with the SpectroCube Arcoptix COTS spectrometer at a resolution of 4 cm^{-1} wavenumbers.

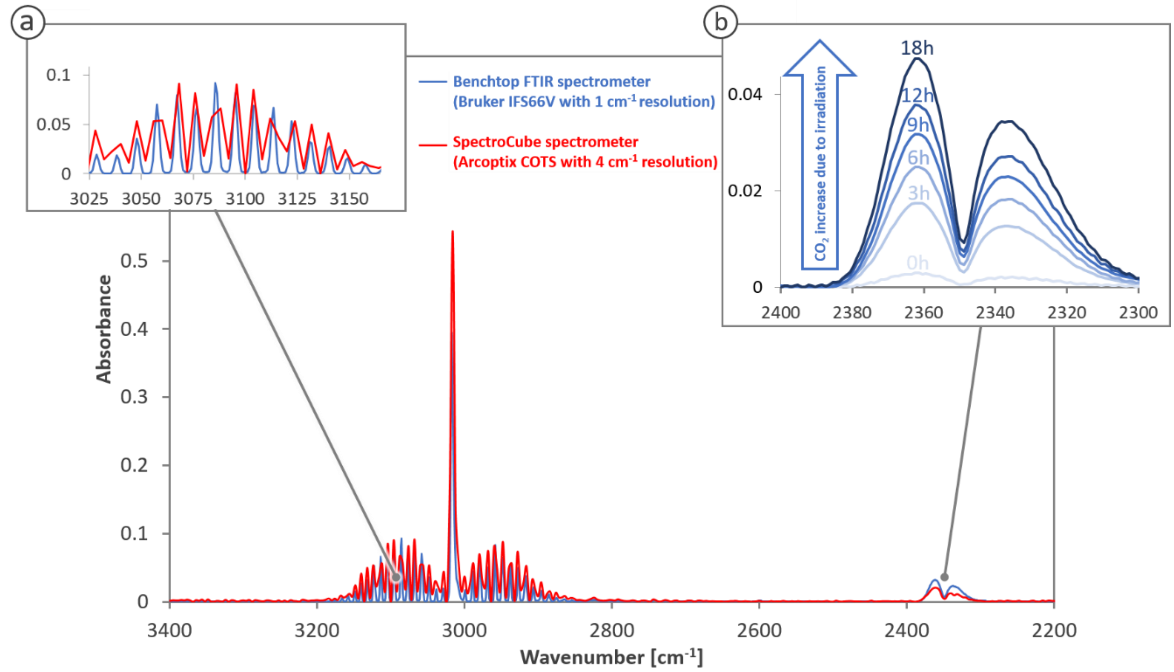

Figure 16: FTIR spectra of a gas cell with 20% methane in nitrogen at atmospheric pressure. A comparison of spectra recorded with a benchtop FTIR spectrometer at 1 cm^{-1} wavenumber resolution and with the SpectroCube Arcoptix COTS spectrometer at 4cm^{-1} resolution (insert a) is shown. Insert b shows CO_2 production due to irradiation of the sample cell with UV light (measured with the Bruker IFS66V instrument).

Additional tests cells were filled with varying concentrations of CO_2, one 100% CO_2 at atmospheric pressure and a cell with 2% CO_2 in Argon. The infrared active bands of CO_2 are located at around 3700, 3600 cm^{-1} and at around 2350 cm^{-1}. The fine structure of the Q-, P- and R-branches require a higher spectral resolution than 1 cm^{-1} and are therefore not visible in the recorded spectra (see figure 17). Additional test samples consisting of various organic thin films (e.g. pigments, lipids, amino acids) were measured to demonstrate that the sample design in combination with the transflection configuration and the selected FTIR spectrometer system is perfectly capable to monitor photochemistry of different states of matter. Gas phase spectra however are more challenging than spectroscopy of thin films and therefore, characterisation of the spectroscopic performance was focused on gas phase spectroscopy. To summarise the test observations, a very good correlation between benchtop FTIR and SpectroCube prototype could be shown and demonstrated the high performance of the selected instrument.

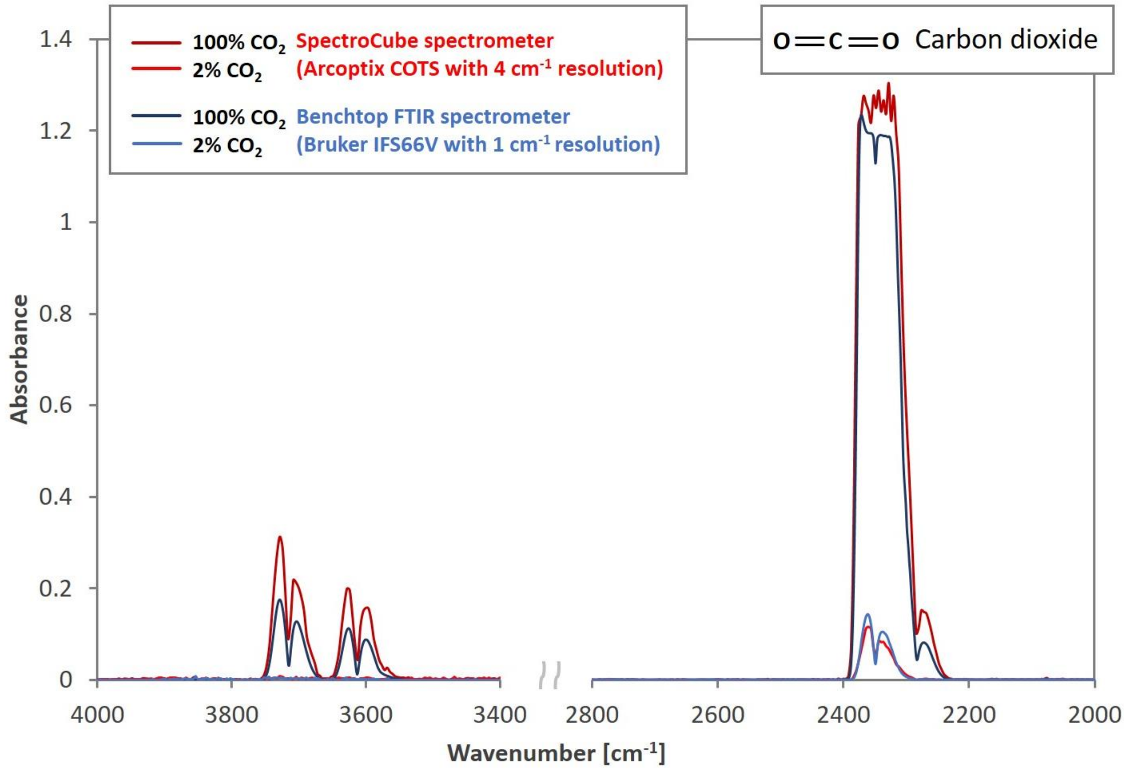

Figure 17: FTIR spectra of CO_2 test cells – a 100% CO_2 cell (darker colours) at atmospheric pressure was compared with a 2% CO_2 cell (lighter colours) in argon and measured with a benchtop FTIR spectrometer at 1 cm^{-1} wavenumber resolution and with the SpectroCube Arcoptix COTS spectrometer at 4 cm^{-1} wavenumber resolution.

5. Conclusion

SpectroCube is an ambitious science and technology demonstration mission that combines miniaturised and modular infrared spectroscopy hardware with a sophisticated, high-capacity and ultra-lightweight sample handling system. With all nanosatellite components required for sun-pointing, attitude control, propulsion, onboard data processing and telemetry fitting inside a 6U CubeSat envelope, SpectroCube will be launched as a free flying nanosatellite into a high elliptical orbit around Earth. The main objective of the here presented feasibility study was to prove that a COTS infrared spectrometer can fulfil the scientific and technological requirements of the SpectroCube project. Based on the spectroscopic performance, the applicable wavelength range, the robustness of the optical system and the level of miniaturisation to fit within a 6U CubeSat envelope, the selected and tested spectrometer is perfectly suited and a very strong candidate for further development into a mission engineering model. The performed vibration and shock testing were extremely important to ensure compliance of the found spectrometer unit with mechanical stress levels experienced by a typical CubeSat payload during launch. Our results show that efficient damping of the interferometer unit can successfully mitigate misalignment and damage to the delicate optical system.

Besides testing of the selected spectroscopic hardware, analysis of potential CubeSat orbits, launch configurations and ground station access demonstrated that the dimensional, mass and power constraints of a 6U CubeSat platform is compatible with a GTO, sGTO or Molniya type orbit, where there are regular and recurrent launch opportunities. These orbits are scientifically of great interest to the SpectroCube mission as an astrobiology/astrochemistry exposure platform because of the expected higher levels of radiation associated with an orbit that stretches beyond the protective magnetic field of LEO.

SpectroCube is a European contribution to increased international efforts aiming at developing interplanetary CubeSats with scientific payloads. Astrobiology and astrochemistry are research fields where the respective scientific community is strongly interested in miniaturised and modular in-situ platforms for exposure experiments in high-radiation space environments. Since radiation is seen as a major obstacle in human space exploration, investigating the effect of solar UV and energetic particle radiation on organic molecules, biomarkers, whole cells and multicellular organisms is a key component in radiation risk mitigation and in developing radiation shielding strategies. SpectroCube belongs to the first pioneering missions to study the interaction of radiation and organic matter on an in-situ infrared spectroscopy 6U CubeSat platform.

Acknowledgements

A. Elsaesser gratefully acknowledges funding by the BMWi/DLR (grant number 50WB1623). A. Elsaesser was supported by the European Union's Horizon 2020 research and innovation programme under the Marie Skłodowska-Curie grant agreement No. 706072 (NanoMembR). The authors would like to thank the ESA CDF study team for the highly constructive and successful design and development process of SpectroCube. This work was supported by the ESA Technology Research Programme (contract No. 4000119981). We thank two anonymous reviewers for critical reading and providing constructive comments, which helped to improve the manuscript.

Declaration of interest

None

References

[1] C.F. Chyba, K.P. Hand, Astrobiology: the study of the living universe, Annu. Rev. Astron. Astrophys., 43 (2005) 31-74.
[2] P. Ehrenfreund, S.B. Charnley, Organic molecules in the interstellar medium, comets, and meteorites: a voyage from dark clouds to the early Earth, Annual Review of Astronomy and Astrophysics, 38 (2000) 427-483.
[3] Y.Y. Guan, N. Fray, P. Coll, F. Macari, D. Chaput, F. Raulin, H. Cottin, UVolution: compared photochemistry of prebiotic organic compounds in low Earth orbit and in the laboratory, Planetary and Space Science, 58 (2010) 1327-1346.
[4] H. Cottin, K. Saiagh, D. Nguyen, N. Grand, Y. Bénilan, M. Cloix, P. Coll, M.-C. Gazaux, N. Fray, D. Khalaf, Photochemical studies in low Earth orbit for organic compounds related to small bodies, Titan and Mars. Current and future facilities, Bulletin de la Société Royale des Sciences de Liège, 84 (2015) 60-73.

[5] K. Woellert, P. Ehrenfreund, A.J. Ricco, H. Hertzfeld, Cubesats: Cost-effective science and technology platforms for emerging and developing nations, Advances in Space Research, 47 (2011) 663-684.
[6] E. Agasid, R. Burton, R. Carlino, G. Defouw, A. Dono Perez, A. Karacahoglu, B. Klamm, A. Rademacher, J. Schalkwyck, R. Shimmin, Small spacecraft technology state of the art, NASA, Ames Research Center, Mission Design Division Rept. NASA/TP-2015-216648/REV1, Moffett Field, CA, (2015).
[7] T. Wekerle, J.B. Pessoa Filho, L.E.V.L.d. Costa, L.G. Trabasso, Status and trends of smallsats and their launch vehicles—An up-to-date review, Journal of Aerospace Technology and Management, 9 (2017) 269-286.
[8] T.H. Zurbuchen, R. von Steiger, S. Bartalev, X. Dong, M. Falanga, R. Fléron, A. Gregorio, T.S. Horbury, D. Klumpar, M. Küppers, Performing High-Quality Science on CubeSats, Space Research Today, 196 (2016) 11-30.
[9] G. Laštovička-Medin, Nano/pico/femto-satellites: Review of challenges in space education and science integration towards disruptive technology, in: Embedded Computing (MECO), 2016 5th Mediterranean Conference on, IEEE, 2016, pp. 357-362.
[10] S.S. Board, E. National Academies of Sciences, Medicine, Achieving Science with CubeSats: Thinking Inside the Box, National Academies Press, 2016.
[11] C. Zuffada, J. Castillo-Rogez, M. Quadrelli, A Consolidated View of Science with SmallSats/CubeSats, in: 42nd COSPAR Scientific Assembly, 2018.
[12] R. Hunter, D.J. Korsmeyer, A Review of NASA Ames CubeSat Program, (2015).
[13] J. Spann, D. Pierce, A. Petro, NASA Perspectives on CubeSat Technology and Highlighted Activities, (2016).
[14] V. Rejsek-Riba, V. Inguimbert, S. Duzellier, C. Pons, M. Crepel, A. Tighe, Spectrometers results of material exposure and degradation experiment onboard international space station, Journal of Spacecraft and Rockets, 48 (2011) 38-44.
[15] N.E. Bramall, R. Quinn, A. Mattioda, K. Bryson, J.D. Chittenden, A. Cook, C. Taylor, G. Minelli, P. Ehrenfreund, A.J. Ricco, The development of the space environment viability of organics (SEVO) experiment aboard the organism/organic exposure to orbital stresses (O/OREOS) satellite, Planetary and Space Science, 60 (2012) 121-130.
[16] A. Elsaesser, R.C. Quinn, P. Ehrenfreund, A.L. Mattioda, A.J. Ricco, J. Alonzo, A. Breitenbach, Y.K. Chan, A. Fresneau, F. Salama, Organics Exposure in Orbit (OREOcube): A Next-Generation Space Exposure Platform, Langmuir, 30 (2014) 13217-13227.
[17] P. Ehrenfreund, A. Ricco, D. Squires, C. Kitts, E. Agasid, N. Bramall, K. Bryson, J. Chittenden, C. Conley, A. Cook, The O/OREOS mission—astrobiology in low Earth orbit, Acta Astronautica, 93 (2014) 501-508.
[18] A. Sgambati, M. Deiml, A. Stettner, J. Kahrs, P. Brozek, P. Kapoun, V. Latini, M. Mariani, E. Rabbow, P. Manieri, SPECTROModule: A modular in-situ spectroscopy platform for Exobiology and Space Sciences, Acta Astronautica, (2019).
[19] A. Marinan, J. Castillo-Rogez, L. Johnson, J. Dervan, C. Seybold, E. Betts, Near Earth Asteroid (NEA) Scout CubeSat Mission, in: 12th Low-Cost Planetary Missions Conference, Pasadena, CA, 2017.
[20] A. Ricco, R. Hanel, S. Bhattacharya, T. Boone, M. Tan, A. Mousavi, A. Rademacher, A. Schooley, B. Klamm, J. Benton, The BioSentinel bioanalytical microsystem: Characterizing DNA radiation damage in living organisms beyond Earth orbit, (2016).
[21] R. Hevner, W. Holemans, J. Puig-Suari, R. Twiggs, An advanced standard for CubeSats, (2011).
[22] S.-E. Qian, Optical payloads for space missions, John Wiley & Sons, 2015.
[23] A. Kuze, H. Suto, K. Shiomi, S. Kawakami, M. Tanaka, Y. Ueda, A. Deguchi, J. Yoshida, Y. Yamamoto, F. Kataoka, Update on GOSAT TANSO-FTS performance, operations, and data products after more than 6 years in space, Atmospheric Measurement Techniques, 9 (2016).
[24] K. Gilbert, D. Turnbull, K. Walker, C. Boone, S. McLeod, M. Butler, R. Skelton, P. Bernath, F. Chateauneuf, M.A. Soucy, The onboard imagers for the Canadian ACE SCISAT-1 mission, Journal of Geophysical Research: Atmospheres, 112 (2007).

[25] A. Harper, M. Ryschkewitsch, A. Obenschain, R. Day, General Environmental Verification Standard (GEVS) for GSFC Flight Programs and Projects, NASA Goddard Space Flight Center, GSFC-STD-7000, (2005).
[26] M. Jonsson, Development of a shock test facility for qualification of space equipment, Department of Applied Mechanics, Göteborg, Sweden, (2012).
[27] D. Smallwood, An improved recursive formula for calculating shock response spectra, shock and vibration Bulletin: Proceedings of the 51st Symposium on Shock and Vibration, San Diego, California, (1980).
[28] R.N. Jones, The effects of chain length on the infrared spectra of fatty acids and methyl esters, Canadian Journal of Chemistry, 40 (1962) 321-333.
[29] Y. Rodríguez-Lazcano, B. Maté, O. Gálvez, V.J. Herrero, I. Tanarro, R. Escribano, Solid L-α-alanine: Spectroscopic properties and theoretical calculations, Journal of Quantitative Spectroscopy and Radiative Transfer, 113 (2012) 1266-1275.